

**Efficient Electrocatalytic Hydrogen Gas Evolution by a
Cobalt-Porphyrin-based Crystalline Polymer**

Journal:	<i>Dalton Transactions</i>
Manuscript ID	DT-ART-01-2018-000302.R2
Article Type:	Paper
Date Submitted by the Author:	01-Jun-2018
Complete List of Authors:	Wu, Yanyu; University of Texas at El Paso, Department of Chemistry Veleta, Jose; The University of Texas at El Paso (UTEP), Chemistry Tang, Diya; Beijing Normal University Price, Alex; The University of Texas at El Paso (UTEP), Physics Botez, Cristian; University of Texas - El Paso, Physics Villagran, Dino; University of Texas at El Paso, Department of Chemistry



Journal Name

ARTICLE

Efficient Electrocatalytic Hydrogen Gas Evolution by a Cobalt-Porphyrin-based Crystalline Polymer

Yanyu Wu,^a José M. Veleta,^a Diya Tang,^b Alex D. Price,^c Cristian E. Botez,^c and Dino Villagrán^{*a}

Received 00th January 20xx,
Accepted 00th January 20xx

DOI: 10.1039/x0xx00000x

www.rsc.org/

Herein we report a crystalline CoTcPP-based [TcPP = the anion of *meso*-tetra(4-carboxyphenyl)porphyrin] polymeric system, **1**, as a hydrogen evolution reaction (HER) electrocatalyst in acidic aqueous media. The material was characterized by powder x-ray diffraction (*p*-XRD), Fourier transform infrared (FT-IR) spectroscopy, energy dispersive x-ray (EDX) analysis and its morphology was probed by scanning electron microscopy (SEM) and transmission electron microscopy (TEM). Polymer **1** shows a surface area of 441.74 m²/g, while the discrete CoTcPP molecule (**2**) shows surface area of 3.44 m²/g. The HER catalytic performance was evaluated by means of linear sweep voltammetry in the presence of 0.5 M H₂SO₄ aqueous solution. To achieve 10 mA/cm² cathodic current density, **1** and **2** respectively require an overpotential of 0.475 V and 0.666 V, providing strong evidence that the extended network of cobalt-based porphyrin leads to enhanced HER efficiency. The polymer also shows great tolerance for HER electrolysis in the presence of acid remaining active over 10 hours.

INTRODUCTION

Hydrogen evolution reactions (HERs) have been proposed as a promising solution for the increasing global energy demand.^{1,2} Exploring electrocatalysts with high efficiency and stability is crucial for the study of HER.^{3,4} Even though platinum metal is well known to be capable of catalyzing the conversion of protons to molecular hydrogen at practical zero overpotential and with large current densities, the design of technologies for large-scale hydrogen production and its commercialization require the use of electrocatalysts made from inexpensive and earth-abundant materials.^{3,5,6} Recently, numerous studies have shown the use of transition metal (Co, Fe, Ni, Mn) based materials as HER electrocatalysts candidates, such as transition metal alloys,^{7–9} chalcogenides,^{10–13} phosphides,^{14,15} transition metal based macrocyclic complexes^{16–18} and metal-free systems.^{19–21} In general, the catalytic systems need to overcome the following three fundamental limitations: (1) high activation energy and slow kinetics of HER; (2) short lifetime of the catalysts to bear constant long-term electrocatalysis; (3) lack of efficient noble-metal free candidates.²²

Metalloporphyrins as HER electrocatalysts have been widely studied and have shown promising results.^{18,23–25} However, they have been mainly studied as homogeneous catalysts, where there is difficulty in separating the electrocatalysts from the substrate. In addition, homogeneous metalloporphyrin

electrocatalysts show poor catalytic performance owing to mass transfer issues and to the limited number of active catalytic sites exposed to the substrate and electrode.²⁶ Therefore, in order to enhance the catalytic performance of these materials, metalloporphyrin-derived heterogeneous HER electrocatalysts have been pursued by increasing the number of exposed catalytic active centers.^{26–28} Porphyrin-based conjugated extended networks have shown to be promising alternatives to molecular systems to yield more active and tolerant heterogeneous catalysts in many important chemical processes such as HER, carbon dioxide and oxygen reduction,^{26–31} among others.^{32–34} The enhanced efficiency of these systems is attributed to higher surface areas that allow for more readily available catalytically active metal sites.^{27,29}

Herein we report a crystalline polymer based on the CoTcPP unit [TcPP = the anion of *meso*-tetra(4-carboxyphenyl)porphyrin]), **1**, as an effective HER electrocatalyst. We present the synthesis and characterization of **1** using standard spectroscopy and microscopy techniques. The polymer was evaluated as a heterogeneous electrocatalyst for hydrogen gas production in a standard acidic aqueous solution (0.5 M H₂SO₄ in water), using electrochemical techniques including linear sweep voltammetry, electrical impedance spectroscopy, bulk electrolysis and chronoamperometry. The discrete molecule CoTcPP (**2**) was also assessed heterogeneously for HER under the same conditions for comparison.

EXPERIMENTAL SECTION

Materials. All reagents were used without further purification unless otherwise stated. 4-carboxybenzaldehyde was purchased from Sigma Aldrich. Co(NO₃)₂·6H₂O and Co(OAC)₂·4H₂O were purchased from Strem Chemicals. H₂SO₄, HCl, MeOH, EtOH, and DMF were obtained from Fisher

^a Department of Chemistry and Biochemistry, The University of Texas at El Paso, El Paso, TX 79968, United States.

^b Department of Chemistry, Beijing Normal University, Beijing 100875, China.

^c Department of Physics, The University of Texas at El Paso, El Paso, TX 79968, United States.

† Footnotes relating to the title and/or authors should appear here.

Electronic Supplementary Information (ESI) available: [details of any supplementary information available should be included here]. See DOI: 10.1039/x0xx00000x

Scientific. Pyrrole was purchased from Acros Organic and was freshly distilled from calcium hydride.

Characterization. ^1H NMR spectroscopy was performed on a Bruker 400 MHz NMR spectrometer, using deuterated DMSO as the solvent and internal calibration. The UV-vis spectra were obtained using a SEC2000 spectra system equipped with a VISUAL SPECTRA 2.1 software. Fourier transform infrared (FT-IR) spectroscopy was recorded on an Agilent Cary 630 FT-IR spectrometer. X-ray diffraction (XRD) was obtained using a PANalytical Empyrean system using Cu-K α radiation ($\lambda = 1.5418 \text{ \AA}$) equipped with a PIXcel [3D] detector. Scanning electron microscope (SEM) images, elemental mapping, and energy dispersive x-ray (EDX) analysis were recorded on a Hitachi S-4800 instrument equipped with an EDX microanalysis system. Transmission electron microscopy was measured on a Hitachi H-7650 instrument.

Synthesis of meso-tetra(4-carboxyphenyl)porphyrin (H_2TcPP). Synthesis was done following a modified literature procedure.³⁵ In a 1 L round bottom flask, 4-carboxybenzaldehyde (5.00g, 33.30 mmol) was dissolved in propionic acid (500 mL) and heated at 140 °C until the mixture was completely dissolved. Then pyrrole (2.23 g, 33.30 mmol) was added dropwise and the mixture was vigorously stirred under reflux for 2 hours. Afterwards, MeOH (100 mL) was added to the reaction and cooled down using an ice bath. The crude product was filtered under reduced pressure using a medium coarse filter frit. The solid residue was washed with deionized water and then dried under reduced pressure to obtain a dark purple powder. Yield: 1.65 g (25.1 %). ^1H NMR (d_6 -DMSO) δ : 13.28 (s, 4H), 8.86 (s, 8H), 8.36 (m, 16H), -2.95 (s, 2H); UV-vis (EtOH): λ max: 419, 519, 552, 592, 648 nm.

Synthesis of crystalline Cobalt meso-tetra(4-carboxyphenyl)porphyrin polymer (1). H_2TcPP (0.0100g, 0.0126 mmol), $\text{Co}(\text{NO}_3)_2 \cdot 6\text{H}_2\text{O}$ (0.0320g, 0.110 mmol) and 5 drops of concentrated HCl were dissolved in 3 mL DMF and 1 mL MeOH in a Pyrex vial. The mixture was sonicated for 30 minutes and then heated at 60 °C in a programmable oven for 72 hours. After cooling down to room temperature, the shiny purple crystals were filtered and cleaned with copious amounts of DMF and MeOH and then dried at 50 °C. Yield: 0.0144 g. UV-vis (pH= 8 buffer in water): λ max: 427, 551 nm. FT-IR (ATR, cm^{-1}) $\nu = 1654$ (w), 1604 (sh, ν^{COO^-}), 1399 (s, ν^{asCOO^-}), 1339 (w), 1278 (w), 1174 (w), 1144 (w), 1000 (sh, Co-N), 838 (s, sh, C-H), 799 (s, sh, aromatic C-H), 771 (s, sh, C-H), 711 (s, sh, C-H). Elemental analysis: C 58.51%; H 3.69%; N 6.76%. Calcd: C 63.87%; H 2.68%; N 6.21%; O 14.18%; Co 13.06%.

Synthesis of Cobalt meso-tetra(4-carboxyphenyl)porphyrin (2). Synthesis was done following a modified literature procedure.³⁵ H_2TcPP (0.100 g, 0.126 mmol) and $\text{Co}(\text{OAc})_2 \cdot 4\text{H}_2\text{O}$ (0.0315 g, 0.126 mmol) were dissolved in DMF (20 mL) and the solution was stirred under reflux for an hour. The reaction mixture was then filtered and the residue was washed with deionized water. Yield: 0.0830 g (80.7%). UV-vis (EtOH): λ max: 429, 546 nm. FT-IR (ATR, cm^{-1}) $\nu = 1720$ (s, sh, C=O), 1684 (s), 1604 (sh, ν^{COO^-}), 1459 (w), 1406 (w, ν^{asCOO^-}), 1263 (s), 1244

(s), 1174 (sh), 1099 (s, sh), 1017 (sh), 1000 (sh, Co-N), 886 (w, C-H), 795 (s, sh, aromatic C-H), 765 (sh, C-H), 728 (s, sh, C-H).

Gas adsorption measurement. Nitrogen adsorption isotherms were obtained using a Micromeritics ASAP 2020 Surface Area and Porosity Analyzer. Samples were weighed and activated for 12 hours at 423 K with an outgas pressure less than 100 mmTorr. N_2 isotherms were measured volumetrically at 77 K, the obtained data and pressure range ($0.0001 \leq P/P_0 \leq 0.1$) was fitted into the Brunauer-Emmett-Teller (BET) equation.

Modification of FTO (fluorinated-tin oxide)/silver working electrodes with 1 and 2. Working electrodes for electrochemical measurements were made by deposition of 1 and 2 using silver glue on FTO glass slides. Prior to the deposition, FTO glass slides were cleaned by sonicating in acetone, isopropanol and deionized water for 10 minutes separately and dried in air. Then 0.5 by 0.5 cm silver paste was coated on top of the active side of the FTO substrate. 2 mg of each catalyst was dispersed in 1 mL ethanol and sonicated for 10 minutes to generate a homogeneous ink. Then 10 μL of the ink was dropcast on top of the silver paste and it was dried in ambient condition (loading mass: 0.08 mg/cm^2).

Electrochemical measurements. Electrochemical data were obtained using a CHI760D potentiostat with a platinum mesh as the counter electrode and saturated calomel electrode (SCE) as the reference electrode in 0.5 M H_2SO_4 aqueous solutions at room temperature. Before each measurement, the solutions were purged with ultra-pure argon gas for 15 minutes to remove the dissolved oxygen. Linear sweep voltammetry experiments were conducted without stirring the solutions. All potentials displayed in the electrochemical experiments are referred to reversible hydrogen electrode (RHE) by adding a value of (0.245 + 0.059 pH) to the data obtained using a SCE reference electrode. Electrical impedance spectroscopy (EIS) was obtained at different overpotentials of 0.25, 0.30, 0.35 and 0.40 V from 100 KHz to 0.1 Hz with AC voltage of 5 mV.

Bulk electrolysis and long-term chronoamperometric measurements were performed in a custom-built two-compartment gas-tight electrochemical cell under an argon atmosphere. The two compartments were separated with a glass frit, where one part of the cell contains the Pt mesh counter electrode and the other compartment contains the working and reference electrodes. The solutions were stirred during the experiment to remove the generated hydrogen gas from the working electrode and the solvent.

Hydrogen gas determination. Hydrogen gas was determined and quantified by a gas chromatograph (GC) after performing bulk electrolysis. The instrument was calibrated by injecting 10%, 20%, 30 % and 40% of ultra-pure hydrogen gas in the GC instrument separately and the concentrations of hydrogen gas are assumed to be proportional to the peak areas. A calibration curve with the correlation of hydrogen gas concentration and peak areas was constructed. Using a gas tight syringe, 50 μL of the gas in the headspace (90 mL) from the cathode side in the two-compartment electrochemical cell was injected to the GC. The percentage of hydrogen gas in the headspace was

determined according to the peak area. The theoretical amount of H_2 was determined by dividing the passed charge (Q) by $2F$ ($F = 96485$). The Faradaic efficiency is calculated according to the following equation:

$$\text{Faradaic efficiency (\%)} = [96485 * 2 * \text{mol } H_2(\text{GC}) * 100] / Q^{36}$$

RESULTS AND DISCUSSION

Figure 1 shows the p -XRD pattern of **1**, revealing its crystallinity by showing a strong and well-defined diffraction peak at $2\theta = 7.47^\circ$ and several other weaker diffraction peaks at $2\theta = 12.80^\circ$, 15.78° , 18.32° and 20.54° , 23.14° and 30.31° respectively. While the diffraction quality of this polymer is not comparable to that of analogous metal-organic frameworks (MOFs),^{26,37,38} clear and well-defined peaks can be observed. Transmission electron microscope (TEM) images (Figures 2a-b) of **1** indicate that this material is composed of thin films. Scanning electron microscope (SEM) images of **1** (Figure 2c-d) shows its irregular cube-like morphology at lower amplifications. The respective elemental mapping images (Figures 2d-f), show the elemental composition of Co, C and O in **1**, which indicate the presence of cobalt centers into the porphyrin crystalline polymer. The presence of Co, C and O in the sample is also confirmed by EDX spectra (Figure S4).

Quantification of the elemental composition of **1** from EDX analysis shows Co, C, N and O contents of 12.38%, 64.97%, 6.84% and 15.81%, respectively. These results deviate from the theoretical values by around 1%, which are small with respect to polymeric systems which typically present much larger deviations.^{39,40,41} Elemental analysis results also show reasonable agreements with respect to theoretical values albeit with larger errors compared to EDX. This is due to the difficulty of the complete combustion of polymers systems and presence of unidentified absorbed gases and solvent in the pores, which have been observed in similar systems.^{40,41}

N_2 sorption measurement through Brunauer-Emmett-Teller (BET) measurements shows a surface area of **1** of ca. 441.74 m^2/g (see Figure 3). In comparison, the CoTcPP monomer, **2**, shows a significantly smaller surface area of 3.44 m^2/g . Thus, the

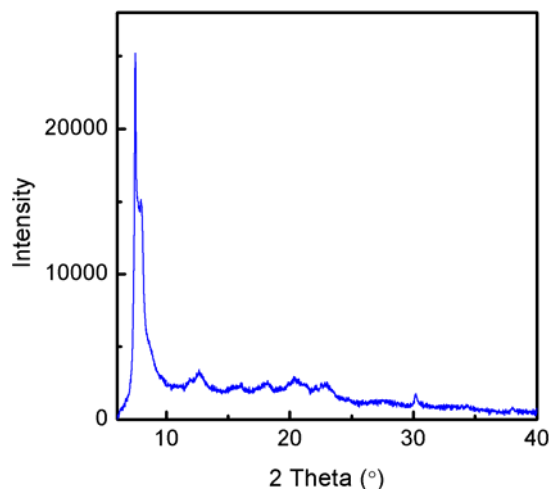


Figure 1. p -XRD pattern of **1**.

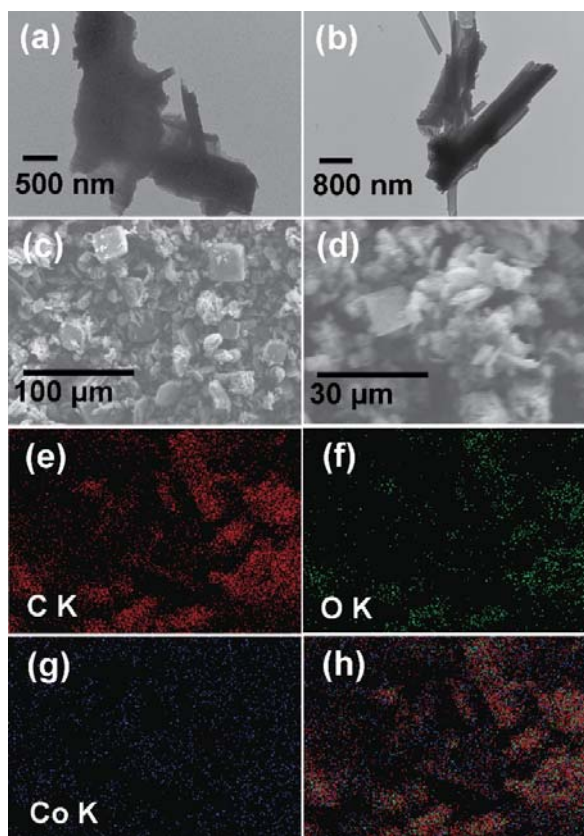


Figure 2. (a-b) TEM images of **1**; (c-d) SEM graphs of **1**; (e-g) the corresponding elemental maps of C, O and Co respectively based on Figure d and (h) overlay elemental mapping image of Co, C and O.

extended network of the crystalline porphyrin polymer, **1**, effectively increases the porosity and surface area of the material, which presumably allows for more exposed active catalytic sites.

The redox activity of the crystalline Co porphyrin-based polymer (**1**) and Co porphyrin monomer (**2**) was studied by cyclic

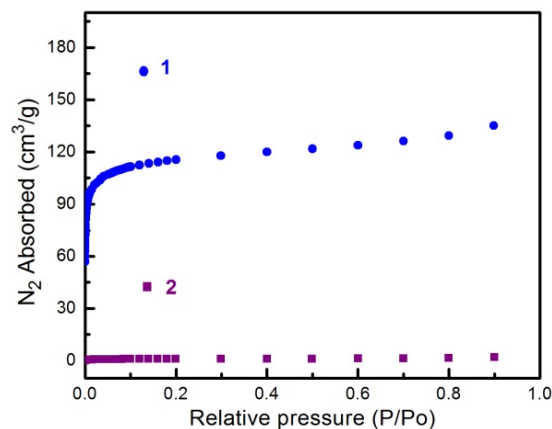


Figure 3. N_2 sorption isotherms at 77 K of **1** and **2**.

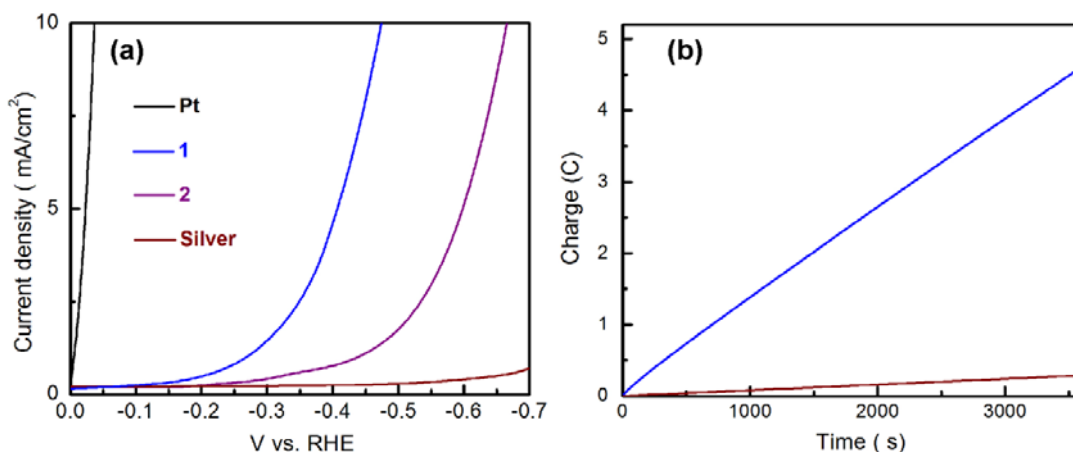


Figure 4. (a) Polarization curves of Pt (black); **1** (blue); **2** (purple); and catalyst-free FTO/Silver (burgundy) in 0.5 M H₂SO₄ electrolyte solution; Scan rate: 2mV/s; (b) Bulk electrolysis measurement of **1** (blue) and catalyst-free FTO/Silver (burgundy) in 0.5 M H₂SO₄ electrolyte solution at a constant applied potential of 0.3 V vs. RHE for an hour.

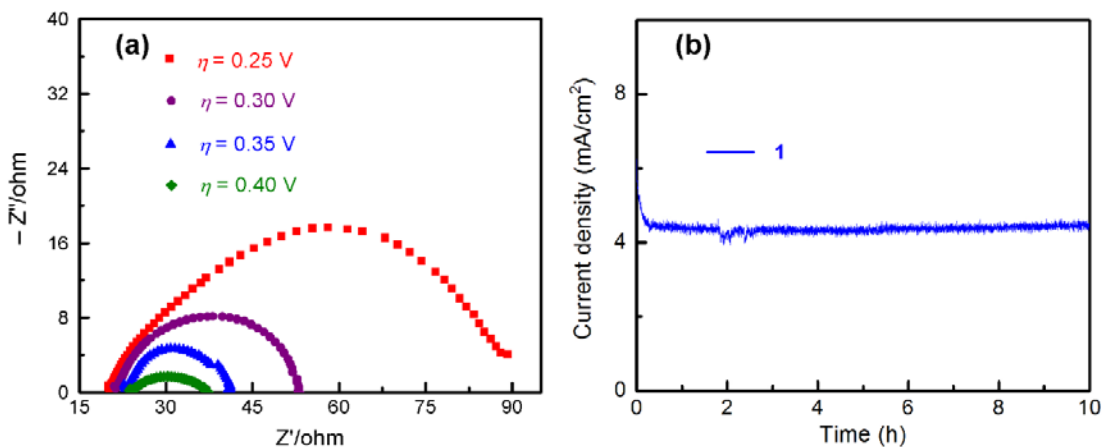


Figure 5. (a) Nyquist plots of the as-prepared **1**/ Silver/FTO electrode at (from top to bottom): $\eta = 0.25, 0.30, 0.35$ and 0.40 V; (b) Chronoamperometric responses ($j \sim t$) of **1** in 0.5 M H₂SO₄ aqueous solution for 10 hours. (Applied potential: -0.4 vs. RHE)

voltammetry in the presence of a pH= 4.56 buffer solution, which can be seen in Figure S6. Polymer **1** and monomer **2** exhibit a reduction event starting at the potential of -0.096 and -0.181 V vs. SCE, respectively. And **1** shows a larger peak current compared to **2**. This result shows that addition of Co to the CoTcPP system help to tune the reduction potential to more anodic value. Linear sweep voltammetry was used to access the HER electrocatalytic properties of **1** and **2**. Both catalysts were evaluated heterogeneously in 0.5 M H₂SO₄ aqueous solution with a scan rate of 2 mV/s. Figure 4a depicts the polarization curves which display the cathodic current as a function of applied potential. As reference, a Pt working electrode (2 mm diameter) and a catalyst-free FTO/silver substrate working electrode were also tested under the same condition. The Pt working electrode exhibits a large cathodic current increase at zero onset overpotential (η) while the FTO/silver working

electrode generates a negligible current increase at the potential range displayed ($0 \sim -0.7$ V vs. RHE). To study the HER

electrocatalytic efficiency, the overpotential (η) was measured at the chosen current density, j , of 10 mA/cm². Electrocatalysts **1** and **2** require an η of 0.475 and 0.666 V, respectively, indicating that the polymeric system exhibits enhanced HER catalytic efficiency by requiring less overpotential when compared to the discrete molecule. This can be explained by the larger surface area that allows more available exposed active sites of the polymer compared to the molecule.

The reaction kinetics of both **1** and **2** as HER electrocatalysts were probed through Tafel plot analysis, where the relationship between η and $\log(j)$ is depicted. The Tafel plots of **1** and **2** are presented in Figure S7. By fitting the plots into the Tafel equation: $\eta = b * \log(j) + a$ (where b is the Tafel slope and a is a constant), Tafel slopes for **1** and **2** are obtained, which are 197 and 264 mV/dec, respectively. Since slower Tafel slopes

correspond to faster kinetics, this result indicates that **1** is a better electrocatalyst than **2**.

The amount of H₂ gas evolved was quantified using a gas chromatograph (GC) after performing bulk electrolysis for an hour. Figure 4b presents the passed charge after an hour's constant electrolysis. The amount of generated H₂ is consistent with the theoretical production based on Faraday's law, assuming all the charges were accounted for the 2 e⁻ reduction of proton to generate H₂, implying quantitative faradaic yield. Electrical impedance spectroscopy (EIS) was conducted to understand the conductivity of the polymeric network. The Nyquist plots of **1** at different η of 0.25, 0.30, 0.35 and 0.40 V, with frequencies ranging from 100 KHz to 0.1 Hz are presented in Figure 5a. The plots show that **1** exhibits good conductivity with relatively small diameters of semicycles. As η increases, the diameters decrease gradually, implying faster HER kinetics at higher η .

To evaluate the durability of the polymer as HER electrocatalyst, long-term chronoamperometric measurement was conducted using the **1**-modified FTO/silver working electrode. Figure 5b exhibits the corresponding current density at a controlled potential of -0.4 V vs. RHE in 0.5 M H₂SO₄ aqueous solution for 10 hours. It can be seen that the catalyst presents excellent catalytic stability under 10 h electrocatalysis with almost no current density decrease. Linear sweep voltammetry using the rinsed catalyst-modified working electrode with the attached catalyst used after 10 h electrolysis in an acid solution of 0.5 M H₂SO₄ (Figure S8) shows an overpotential increase of ca. 5 mV at 10 mA/cm² which implies minimum catalyst leaching over long term electrolysis.

Conclusions

We have compared a crystalline cobalt porphyrin-based polymer and a cobalt porphyrin monomer for electrocatalytic hydrogen gas generation in strong acidic media. The polymer shows significantly larger surface area and enhanced catalytic performance compared to the discrete molecule. This gives strong evidence that by constructing a polymeric system based on HER electrocatalytic active molecular catalysts can increase the surface area to therefore enhance the catalytic efficiency.

Conflicts of interest

The authors declare no conflicts of interest.

Acknowledgements

This work was supported by NSF under award number CHE-1305124. And we thank Prof. Geoffrey B. Saupe and Tahmina Akter for access to the GC instrument.

Notes and references

- M. G. Walter, E. L. Warren, J. R. McKone, S. W. Boettcher, Q. Mi, E. A. Santori and N. S. Lewis, *Chem. Rev.*, 2010, **110**, 6446–6473.
- J. A. Turner, *Science*, 2004, **305**, 972–974.
- H. B. Gray, *Nat. Chem.*, 2009, **1**, 7–7.
- N. S. Lewis and D. G. Nocera, *Proc. Natl. Acad. Sci.*, 2006, **103**, 15729–15735.
- C. G. Morales-Guio, L.-A. Stern and X. Hu, *Chem. Soc. Rev.*, 2014, **43**, 6555–6569.
- M.-R. Gao, J.-X. Liang, Y.-R. Zheng, Y.-F. Xu, J. Jiang, Q. Gao, J. Li and S.-H. Yu, *Nat. Commun.*, DOI:10.1038/ncomms6982.
- J. R. McKone, B. F. Sadler, C. A. Werlang, N. S. Lewis and H. B. Gray, *ACS Catal.*, 2013, **3**, 166–169.
- Y. Shen, Y. Zhou, D. Wang, X. Wu, J. Li and J. Xi, *Adv. Energy Mater.*, 2018, **8**, n/a-n/a.
- S. Wang, J. Wang, M. Zhu, X. Bao, B. Xiao, D. Su, H. Li and Y. Wang, *J. Am. Chem. Soc.*, 2015, **137**, 15753–15759.
- B. Hinnemann, P. G. Moses, J. Bonde, K. P. Jørgensen, J. H. Nielsen, S. Horch, I. Chorkendorff and J. K. Nørskov, *J. Am. Chem. Soc.*, 2005, **127**, 5308–5309.
- T. F. Jaramillo, K. P. Jørgensen, J. Bonde, J. H. Nielsen, S. Horch and I. Chorkendorff, *Science*, 2007, **317**, 100–102.
- D. Merki, H. Vrubel, L. Rovelli, S. Fierro and X. Hu, *Chem. Sci.*, 2012, **3**, 2515–2525.
- Y. Wu, M. Zarei-Chaleshtori, B. Torres, T. Akter, C. Diaz-Moreno, G. B. Saupe, J. A. Lopez, R. R. Chianelli and D. Villagrán, *Int. J. Hydrog. Energy*, 2017, **42**, 20669–20676.
- J. F. Callejas, C. G. Read, E. J. Popczun, J. M. McEnaney and R. E. Schaak, *Chem. Mater.*, 2015, **27**, 3769–3774.
- L. Feng, H. Vrubel, M. Bensimon and X. Hu, *Phys. Chem. Chem. Phys.*, 2014, **16**, 5917–5921.
- X. Hu, B. S. Brunshwig and J. C. Peters, *J. Am. Chem. Soc.*, 2007, **129**, 8988–8998.
- J. L. Dempsey, B. S. Brunshwig, J. R. Winkler and H. B. Gray, *Acc. Chem. Res.*, 2009, **42**, 1995–2004.
- C. C. L. McCrory, C. Uyeda and J. C. Peters, *J. Am. Chem. Soc.*, 2012, **134**, 3164–3170.
- Y. Wu, N. Rodríguez-López and D. Villagrán, *Chem. Sci.*, DOI:10.1039/C8SC00093J.
- B. C. Patra, S. Khilari, R. N. Manna, S. Mondal, D. Pradhan, A. Pradhan and A. Bhaumik, *ACS Catal.*, 2017, **7**, 6120–6127.
- S. Bhunia, S. K. Das, R. Jana, S. C. Peter, S. Bhattacharya, M. Addicoat, A. Bhaumik and A. Pradhan, *ACS Appl. Mater. Interfaces*, 2017, **9**, 23843–23851.
- J. Staszak-Jirkovský, C. D. Malliakas, P. P. Lopes, N. Danilovic, S. S. Kota, K.-C. Chang, B. Genorio, D. Strmcnik, V. R. Stamenkovic, M. G. Kanatzidis and N. M. Markovic, *Nat. Mater.*, 2016, **15**, 197–203.
- I. Bhugun, D. Lexa and J.-M. Savéant, *J. Am. Chem. Soc.*, 1996, **118**, 3982–3983.
- C. H. Lee, D. K. Dogutan and D. G. Nocera, *J. Am. Chem. Soc.*, 2011, **133**, 8775–8777.
- B. B. Beyene, S. B. Mane and C.-H. Hung, *Chem. Commun.*, 2015, **51**, 15067–15070.
- I. Hod, M. D. Sampson, P. Deria, C. P. Kubiak, O. K. Farha and J. T. Hupp, *ACS Catal.*, 2015, **5**, 6302–6309.
- H. Jia, Y. Yao, Y. Gao, D. Lu and P. Du, *Chem. Commun.*, 2016, **52**, 13483–13486.
- S. Cui, M. Qian, X. Liu, Z. Sun and P. Du, *ChemSusChem*, 2016, **9**, 2365–2373.
- Z.-S. Wu, L. Chen, J. Liu, K. Parvez, H. Liang, J. Shu, H. Sachdev, R. Graf, X. Feng and K. Müllen, *Adv. Mater.*, 2014, **26**, 1450–1455.

ARTICLE

Journal Name

- 30 G. Mukherjee, J. Thote, H. Barike Aiyappa, S. Kandambeth, S. Banerjee, K. Vanka and R. Banerjee, *Chem. Commun.*, 2017, **53**, 4461–4464.
- 31 S. Brüller, H.-W. Liang, U. I. Kramm, J. W. Krumpfer, X. Feng and K. Müllen, *J. Mater. Chem. A*, 2015, **3**, 23799–23808.
- 32 L. Chen, Y. Yang and D. Jiang, *J. Am. Chem. Soc.*, 2010, **132**, 9138–9143.
- 33 A. Chen, Y. Zhang, J. Chen, L. Chen and Y. Yu, *J. Mater. Chem. A*, 2015, **3**, 9807–9816.
- 34 A. R. Oveisi, K. Zhang, A. Khorramabadi-zad, O. K. Farha and J. T. Hupp, *Sci. Rep.*, 2015, **5**, 10621.
- 35 H. Shahroosvand, S. Zakavi, A. Sousaraei, E. Mohajerani and M. Mahmoudi, *Dalton Trans.*, 2015, **44**, 8364–8368.
- 36 J. G. Kleingardner, B. Kandemir and K. L. Bren, *J. Am. Chem. Soc.*, 2014, **136**, 4–7.
- 37 D. D. La, H. P. N. Thi, Y. S. Kim, A. Rananaware and S. V. Bhosale, *Appl. Surf. Sci.*, 2017, **424**, 145–150.
- 38 J. Park, Q. Jiang, D. Feng, L. Mao and H.-C. Zhou, *J. Am. Chem. Soc.*, 2016, **138**, 3518–3525.
- 39 G. Liu, Y. Wang, C. Shen, Z. Ju and D. Yuan, *J. Mater. Chem. A*, 2015, **3**, 3051–3058.
- 40 S. Yao, X. Yang, M. Yu, Y. Zhang and J.-X. Jiang, *J. Mater. Chem. A*, 2014, **2**, 8054–8059.
- 41 Y. Liu, S. Wu, G. Wang, G. Yu, J. Guan, C. Pan and Z. Wang, *J. Mater. Chem. A*, 2014, **2**, 7795–7801.